

## Electronic Supporting Information

### Controlling Release Kinetics of pH-Responsive Polymer Nanoparticles

Naruphorn Dararatana, Farzad Seidi, Juliette Hamel, and Daniel Crespy \*

Department of Materials Science and Engineering, School of Molecular Science and Engineering, Vidyasirimedhi Institute of Science and Technology (VISTEC), Rayong 21210, Thailand

E-mail: [daniel.crespy@vistec.ac.th](mailto:daniel.crespy@vistec.ac.th)

### Material and methods

#### Materials

*n*-Butyl methacrylate (BMA, >99%, TCI chemical) and glycidyl methacrylate (GMA, >97%, Sigma-Aldrich) were purified by distillation before using. Toluene (99.8%, Carlo Erba), toluene extra dry (99.85%, Acros Organics), dichloromethane (DCM, 99.9%, Carlo Erba), 1,4-dioxane (99.8%, Carlo Erba), tetrahydrofuran (THF, >99.8%, Carlo Erba), diisopropyl ether (99%, Carlo Erba), diethyl ether stabilized with BHT (99.7%, AppliChem), *N,N*-dimethylformamide (DMF, 99.8%, Carlo Erba), ethanol absolute anhydrous (99.9%, Carlo Erba), tryptamine (>98%, TCI chemical), 8-hydroxyquinoline (>99%, TCI chemical), triphenylphosphine (99%, Acros Organics) 4-hydroxybenzaldehyde (99%, Acros Organics), copper (I) bromide extra pure (98%, Acros Organics), methyl  $\alpha$ -bromoisobutyrate ( $\geq$ 99%, Sigma-Aldrich), 2,2'-dipyridyl (bpy, >99%, Acros Organics), benzotriazole-5-carboxylic acid (99%, Sigma-Aldrich), thionyl chloride (>98%, TCI chemical), hydrazine monohydrate (98%, TCI chemical), hydrochloric acid (37%, Carlo Erba), formaldehyde (37%, Quality Reagent Chemical), potassium carbonate (99%, Carlo Erba), zinc chloride (>98%, Carlo Erba), sodium azide ( $\geq$ 99.5%, Carlo Erba), methacrylic anhydride (99%, Sigma-Aldrich), 2-(dimethylamino)pyridine (DMAP, 97%, Sigma-Aldrich), sodium dodecyl sulfate (SDS, 99%, Acros Organics), cetyltrimethylammonium bromide (CTAB, 99%, Acros Organics), 1,1'-azobis(cyclohexanecarbonitrile) (ABCN, 98%, Sigma-Aldrich), dimethyl sulfoxide- $D_6$  (99.9%, Cambridge Isotope Laboratories), chloroform- $D$  ( $CDCl_3$ , 99.8%, Cambridge Isotope Laboratories) and deuterium oxide ( $D_2O$ , 99.96%, Cambridge Isotope Laboratories) were used without further purification.

### 1. Synthesis of ethyl benzotriazole-5-carboxylate (BTA-COOEt)

Benzotriazole-5-carboxylic acid (5.0 g, 30.65 mmol) was dissolved in 15 mL of absolute ethanol in a 50 mL round-bottom flask and cooled by stirring in an ice bath for 5 min. Then, thionyl chloride (11.0 g, 92.46 mmol) was slowly dropped into the stirring mixture, and the reaction mixture was heated in a round bottom flask equipped with a reflux condenser at 85 °C while stirring for 8 h. The solution was added dropwise with continuous stirring to 100 mL of cold saturated NaHCO<sub>3</sub> and the product was extracted by ethyl acetate (3x50 mL). The organic phase was dried over Na<sub>2</sub>SO<sub>4</sub> and the solvent was evaporated using rotary evaporator to give 5.8 g of product as a light brown powder (99% yield). <sup>1</sup>H NMR (600 MHz, CDCl<sub>3</sub>, δ): 1.57 (t, J = 8.1 Hz, 3H; CH<sub>3</sub>), 4.49 (m, J = 7.0 Hz, 2H; CH<sub>2</sub>), 7.93 (d, J = 8.65 Hz, 1H; Ar), 8.23 (d, J = 8.63 Hz, 1H; Ar), 8.77 (s, 1H, Ar). HRMS m/z: [M+H]<sup>+</sup> calcd for C<sub>9</sub>H<sub>9</sub>N<sub>3</sub>O<sub>2</sub> 192.0768; found 192.0771.

### 2. Synthesis of benzo-triazole-5-carbohydrazide (BTA hydrazide)

BTA-COOEt (5.8 g, 30.34 mmol) in 30 mL absolute ethanol was cooled in an ice bath and then a solution of hydrazine monohydrate (16.51 g, 33.02 mmol) in 50 mL absolute ethanol was added. The mixture was refluxed at 85 °C for 9 h. The product was precipitated during the reaction and the solvent was removed in a rotary evaporator. The crude product was purified by stirring in 50 mL absolute ethanol, filtrated through filtration paper, and dried in vacuum to provide 5.0 g of pure product as light brown powder (92% yield). <sup>1</sup>H NMR (600 MHz, DMSO-D<sub>6</sub>, δ): 5.47 (s, 2H; NH<sub>2</sub>), 7.73 (d, J = 8.52 Hz, 1H; Ar), 7.81 (d, J = 8.58 Hz, 1H; Ar), 8.33 (s, 1H, Ar). HRMS m/z: [M+H]<sup>+</sup> calcd for C<sub>7</sub>H<sub>7</sub>N<sub>5</sub>O 178.0723; found 178.0715.

### 3. Synthesis of 5-chloromethyl-8-hydroxyquinoline

8-hydroxyquinoline (29 g, 0.2 mol) mixed with 140 mL of concentrated hydrochloric acid and 37% formaldehyde (18.29 mL, 0.66 mol) were treated with zinc chloride (1.8 g, 0.013 mol) and stirred overnight. The mixture was filtered, washed with acetone and dried to provide 34 g (90% yield) of pure product as yellowish solid. <sup>1</sup>H NMR (600 MHz, D<sub>2</sub>O, δ, Fig. S1): 5.00 (s, 2H; CH<sub>2</sub>), 7.32 (d, J = 6.42 Hz, 1H; Ar), 7.66 (d, j = 6.36 Hz, 1H; Ar), 8.04 (s, 1H, Ar), 8.95 (s, 1H, Ar), 9.20 (d, J = 7.74 Hz, 1H; Ar).

#### 4. Synthesis of 5-(azidomethyl)-8-hydroxyquinoline

5-chloromethyl-8-hydroxyquinoline (34 g, 0.18 mol) was dissolved in 200 mL DMF, and then  $\text{NaN}_3$  (59 g, 0.9 mol) was directly added to the mixture. The reaction was stirred at 70 °C for 24 h. After cooling the mixture, the solvent was evaporated with a rotary evaporator and the residue was treated with 100 mL chloroform and 50 mL deionized water. The product was dissolved in the organic phase, was washed one more time with deionized water (20 mL), and then dried over  $\text{MgSO}_4$ . The solvent was concentrated with a rotary evaporator and purified by recrystallization from ethanol to provide 32 g (90% yield) of pure product as light yellow solid.  $^1\text{H}$  NMR (600 MHz,  $\text{CDCl}_3$ ,  $\delta$ , Fig.S2): 4.67 (s, 2H;  $\text{CH}_2$ ), 7.16 (d,  $J = 7.68$  Hz, 1H; Ar), 7.46 (d,  $J = 7.68$  Hz, 1H; Ar), 7.55 (m,  $J = 4.16$  Hz, 1H; Ar), 8.39 (d,  $J = 8.46$  Hz, 1H; Ar), 8.86 (d,  $J = 3.84$  Hz, 1H; Ar).

#### 5. Synthesis of 5-(aminomethyl)-8-hydroxyquinoline (AM8HQ)

A mixture of 5-(azidomethyl)-8-hydroxyquinoline (32 g, 0.16 mol) in 500 mL of THF was treated with  $\text{PPh}_3$  (83.93 g, 0.32 mol) and stirred at room temperature for 10 h. Then, 30 mL of deionized water was added, and the reaction was continued for 6 h. The mixture was concentrated with a rotary evaporator and the residue was precipitated with 100 mL diethyl ether. The obtained product was filtered, washed with (3x50 mL) cold diethyl ether, and then dried under vacuum at room temperature. Column chromatography purification on silica gel with a mixture hexane:THF (1:4) provided 15.15 g (54% yield) of a yellowish solid.  $^1\text{H}$  NMR (600 MHz,  $\text{CDCl}_3$ ,  $\delta$ , Fig.S3): 5.47 (s, 2H;  $\text{CH}_2$ ), 7.14 (d,  $J=7.74$  Hz, 1H; Ar), 7.44 (d,  $J=7.68$  Hz, 1H; Ar), 7.52 (m,  $J=4.16$  Hz, 1H; Ar), 8.50 (d,  $J=8.46$  Hz, 1H; Ar), 8.82 (d,  $J=3.30$  Hz, 1H; Ar). HRMS  $m/z$ :  $[\text{M}+\text{H}]^+$  calcd for  $\text{C}_{10}\text{H}_{10}\text{N}_2\text{O}$  175.0866; found 175.0880.

#### 6. Synthesis of 4-formylphenyl methacrylate (FPMA)

4-hydroxybenzaldehyde (1.5 g, 12.3 mmol), DMAP (0.15 g, 1.2 mmol), and triethylamine (3.1 g, 30.7 mmol) were dissolved in 12 mL of chloroform in a 25 mL of round bottom flask. The flask was cooled to 0 °C and stirred under nitrogen for 15 min. Methacrylic anhydride (4.73 g, 30.7 mmol) was added dropwise and the reaction

mixture was allowed to warm up to room temperature and stirred for 24 h. The crude product was washed twice with deionized water, then twice with a saturated solution of  $\text{NaHCO}_3$ , and one last time with deionized water. The organic solution was dried over  $\text{MgSO}_4$ . Afterwards, it was filtrated through a piece of cotton and the solvent was removed with a rotary evaporator. The product was purified by column chromatography on silica gel (EtOAc: pentane 1:19) to obtain a light brown powder (99% yield).  $^1\text{H}$  NMR (600 MHz,  $\text{CDCl}_3$ ,  $\delta$ , Fig. S4): 2.06 (t,  $J=20.49$  Hz, 3H;  $\text{CH}_3$ ), 5.83 (s, 1H;  $\text{CH}_2$ ), 6.40 (s, 1H;  $\text{CH}_2$ ), 7.34 (d,  $J=7.86$  Hz, 2H; Ar), 7.96 (d,  $J=7.86$  Hz, 2H; Ar), 10.02 (s, 1H; CHO).

## NMR spectra

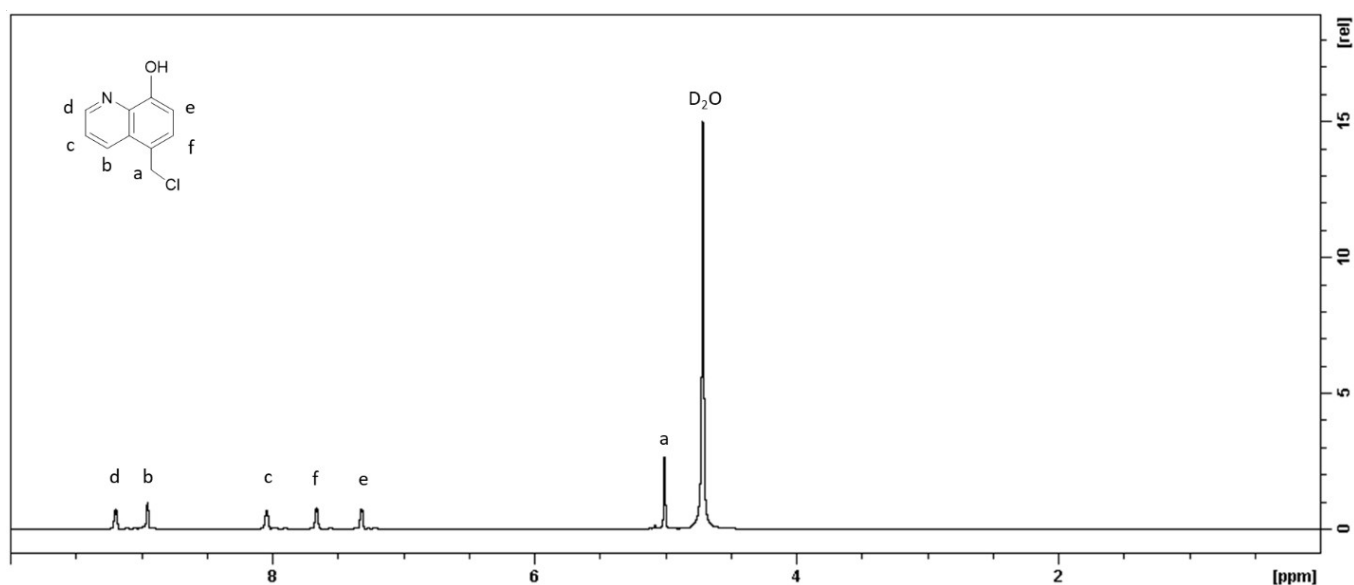


**Figure S1.**  $^1\text{H}$ -NMR spectrum of 5-chloromethyl-8-hydroxyquinoline in  $\text{D}_2\text{O}$

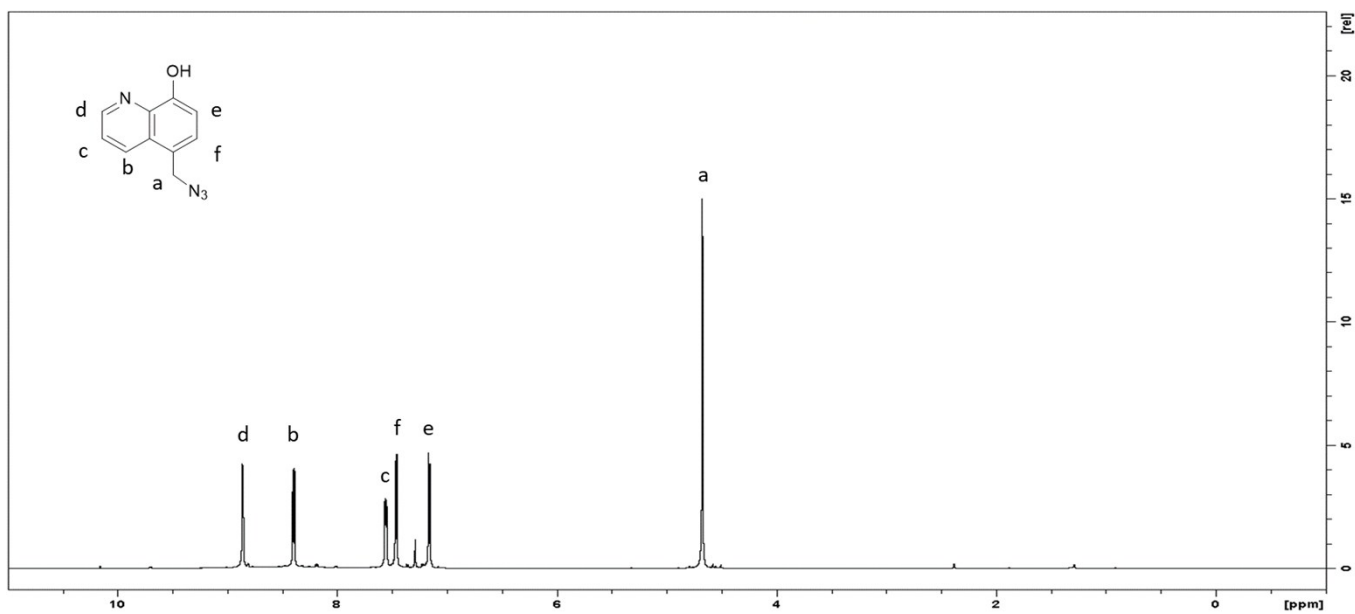


**Figure S2.** <sup>1</sup>H-NMR spectrum of 5-(azidomethyl)-8-hydroxyquinoline in CDCl<sub>3</sub>

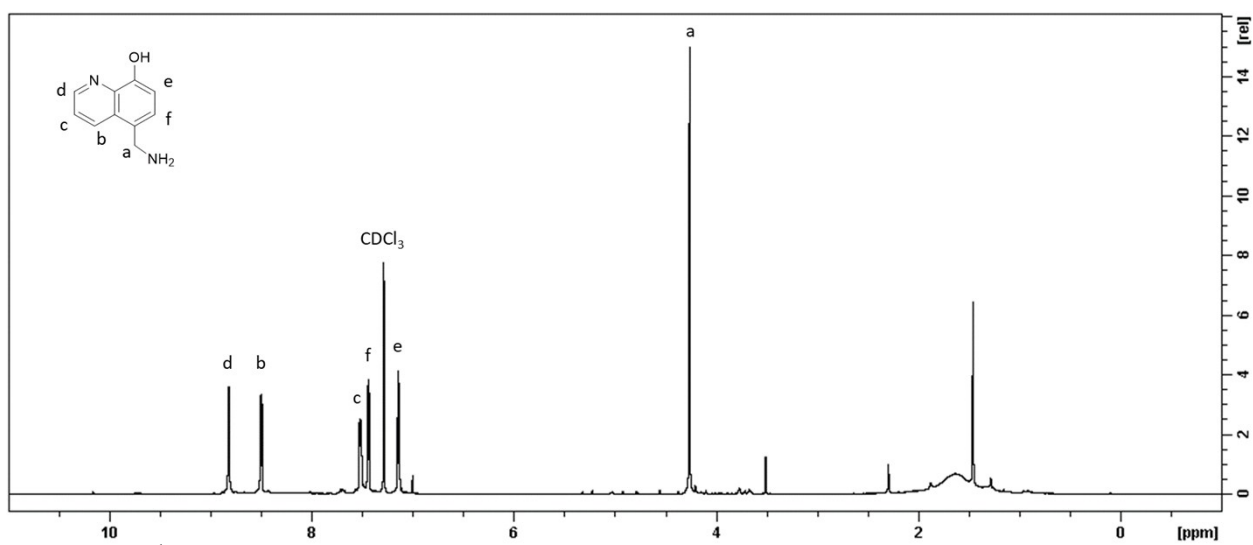


**Figure S3.** <sup>1</sup>H-NMR spectrum of 5-(aminomethyl)-8-hydroxyquinoline (AM8HQ) in CDCl<sub>3</sub>

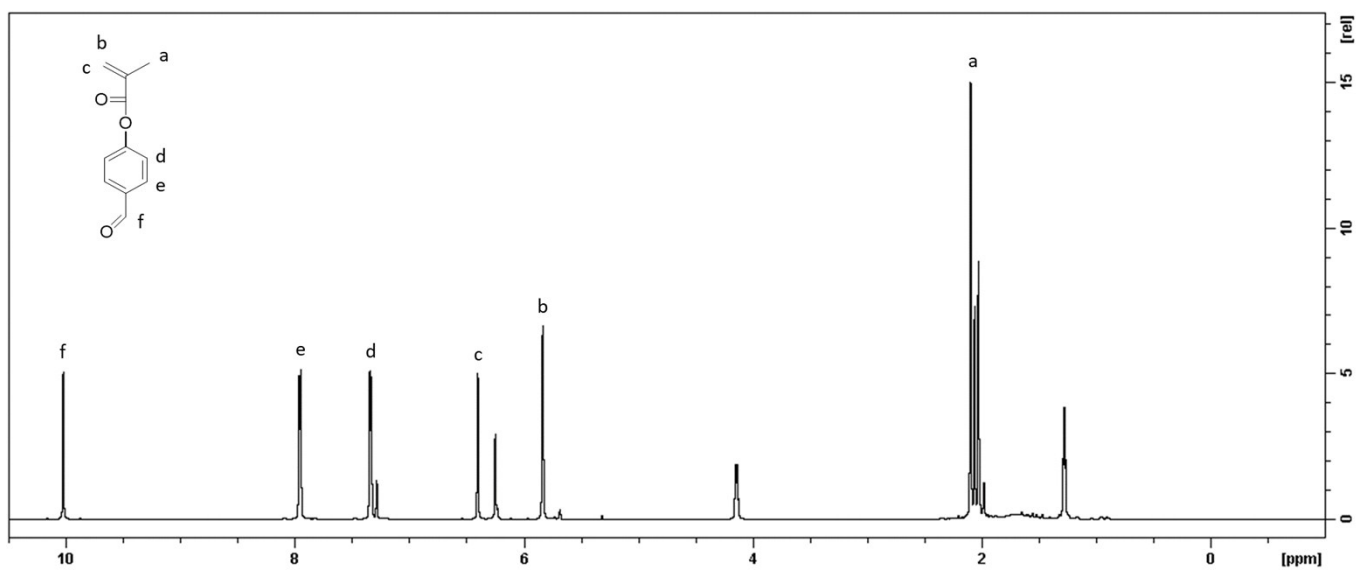


**Figure S4.** <sup>1</sup>H-NMR spectrum of 4-formylphenyl methacrylate (FPMA) in CDCl<sub>3</sub>

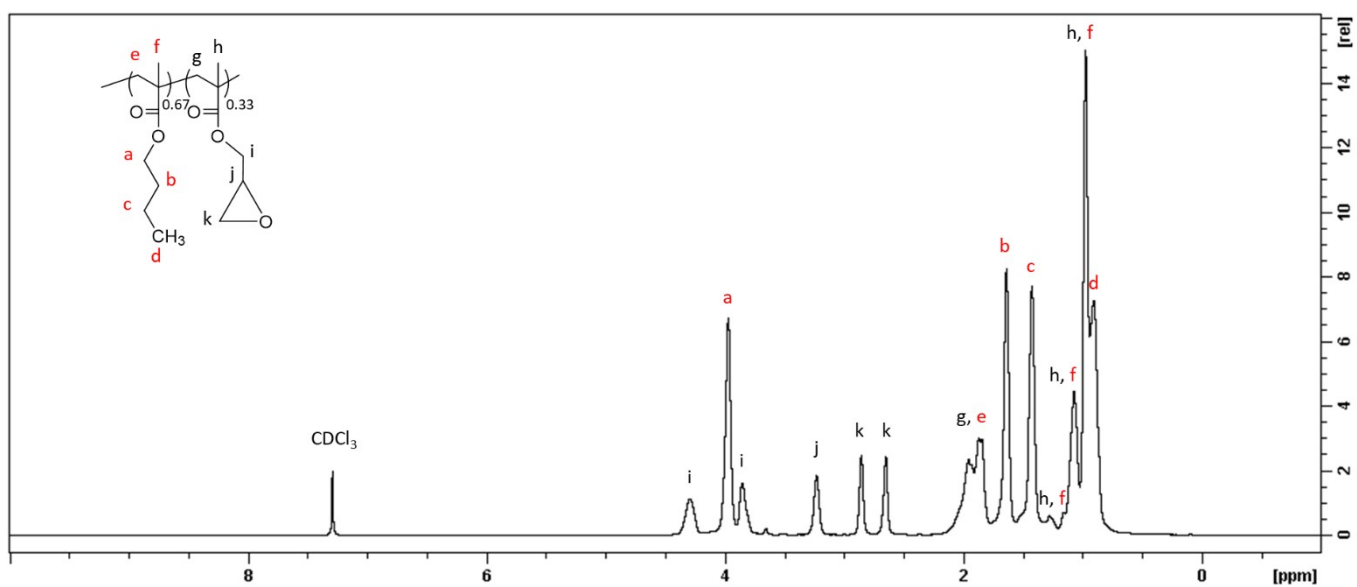


**Figure S5.** <sup>1</sup>H-NMR spectrum of poly[(*n*-butyl methacrylate)<sub>0.67</sub>-*co*-(glycidyl methacrylate)<sub>0.33</sub>] (P1) in CDCl<sub>3</sub>.

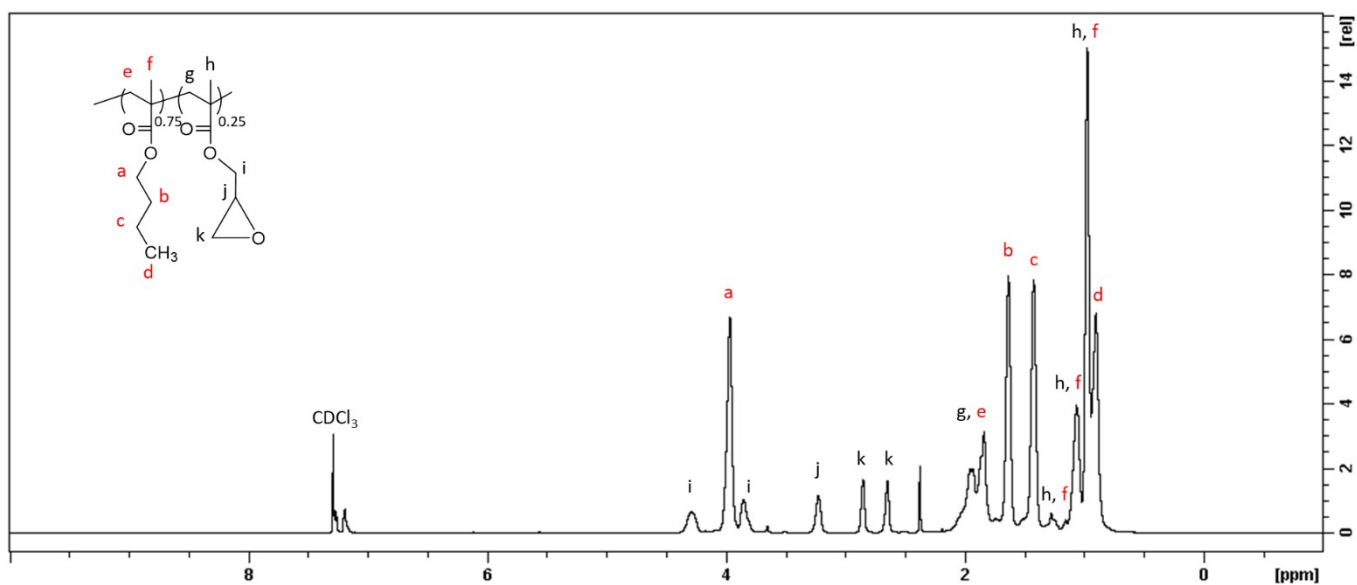


**Figure S6.** <sup>1</sup>H-NMR spectrum of poly[(*n*-butyl methacrylate)<sub>0.75</sub>-*co*-(glycidyl methacrylate)<sub>0.25</sub>] (P2) in CDCl<sub>3</sub>.

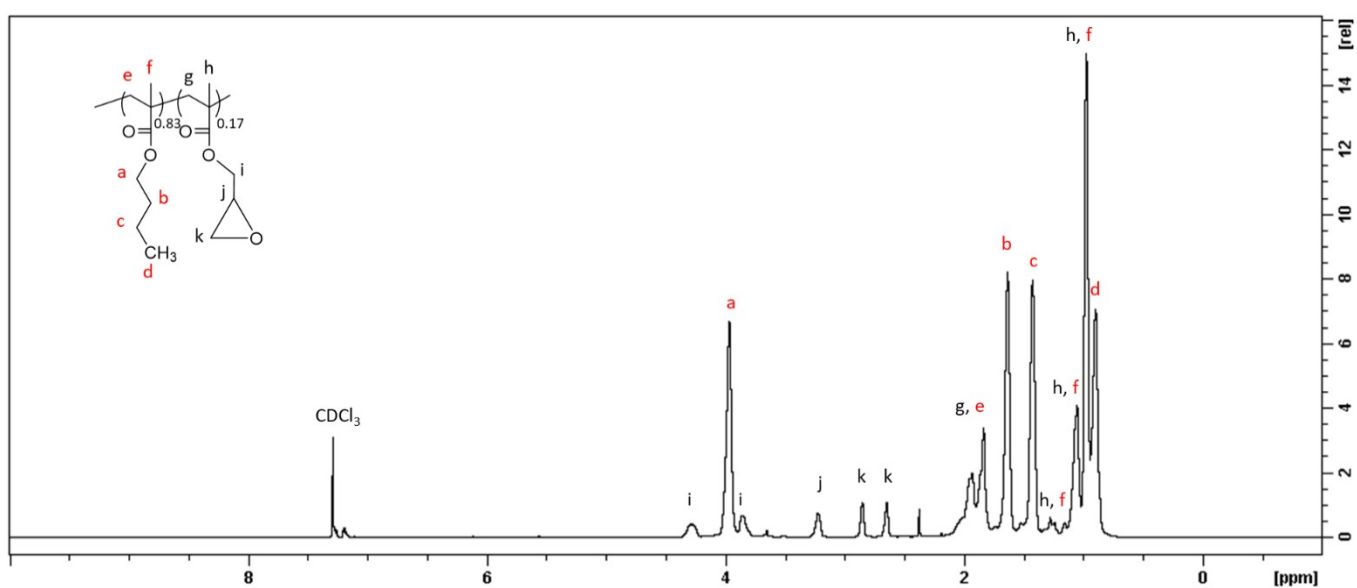


**Figure S7.** <sup>1</sup>H-NMR spectrum of poly[(*n*-butyl methacrylate)<sub>0.83</sub>-*co*-(glycidyl methacrylate)<sub>0.17</sub>] (P3) in CDCl<sub>3</sub>.

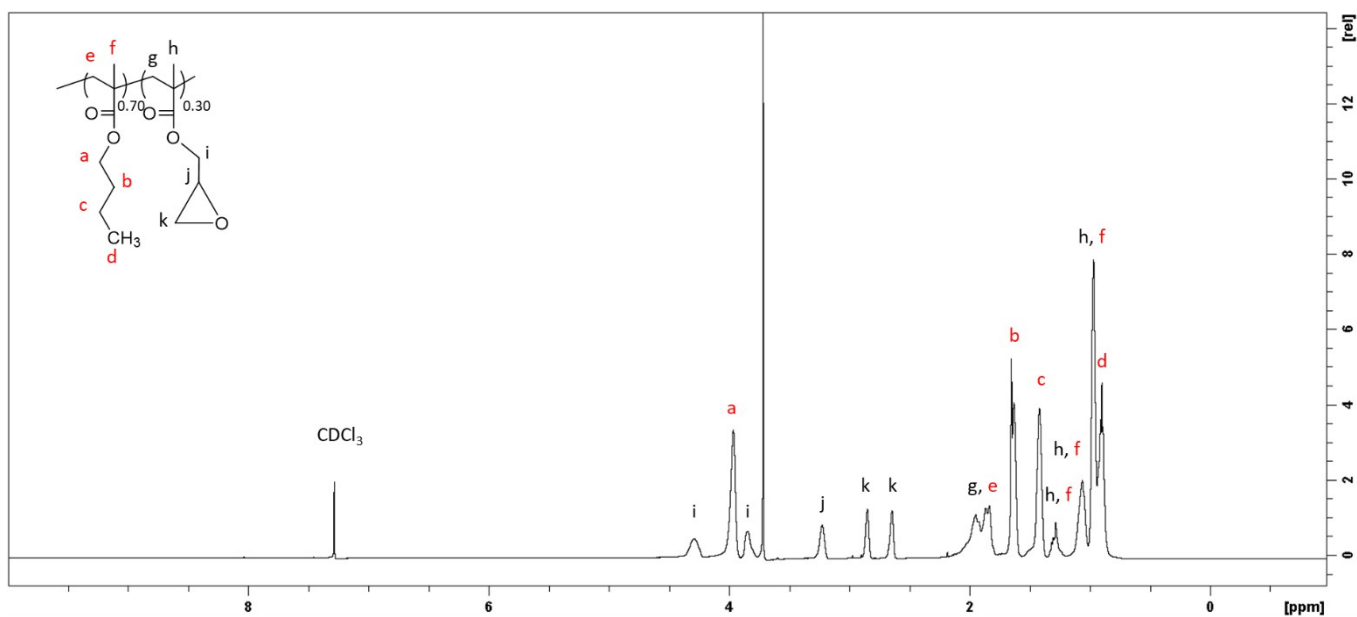


**Figure S8.** <sup>1</sup>H-NMR spectrum of poly[(*n*-butyl methacrylate)<sub>0.70</sub>-*co*-(glycidyl methacrylate)<sub>0.30</sub>] (P4) in CDCl<sub>3</sub>.

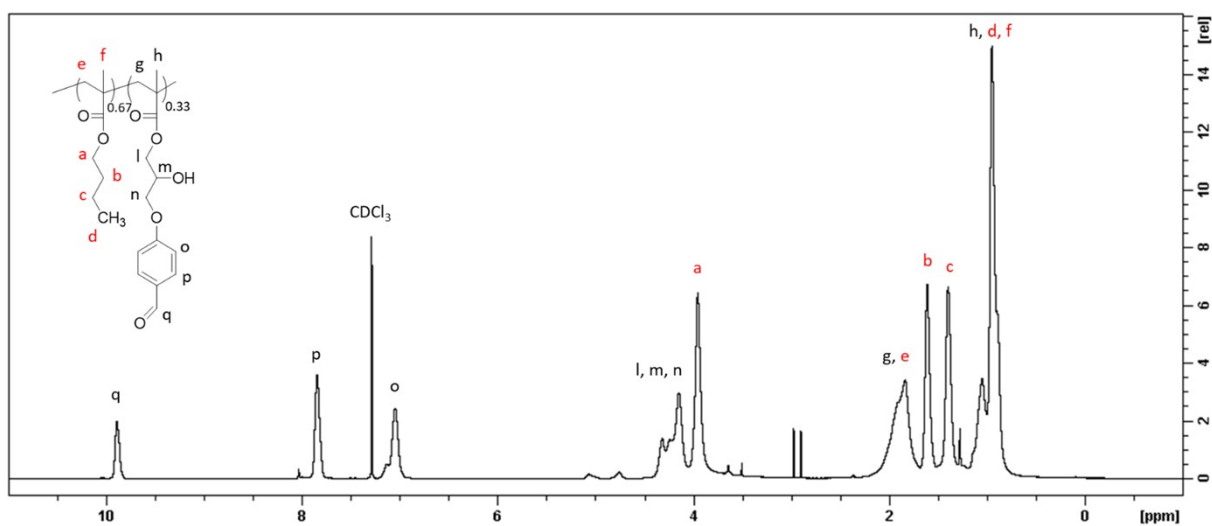


**Figure S9** <sup>1</sup>H-NMR spectrum of aldehyde modified poly[(*n*-butyl methacrylate)<sub>0.67</sub>-*co*-(glycidyl methacrylate benzaldehyde)<sub>0.33</sub>] (P1') in CDCl<sub>3</sub>.

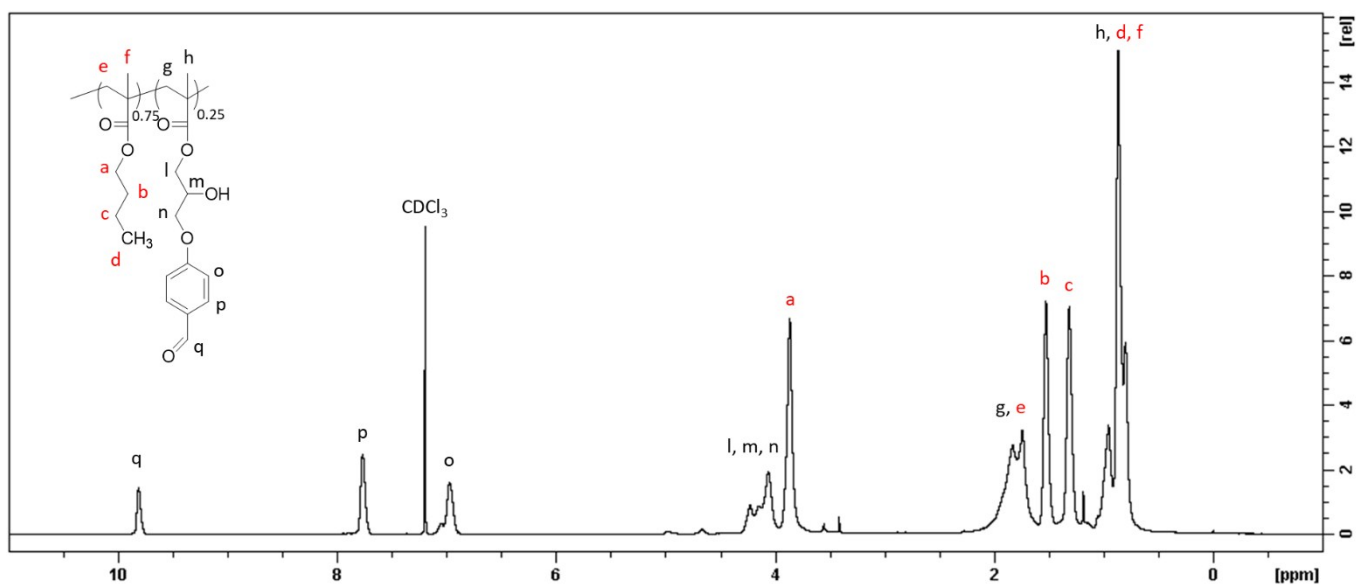


**Figure S10.** <sup>1</sup>H-NMR spectrum of aldehyde modified poly[(*n*-butyl methacrylate)<sub>0.75</sub>-*co*-(glycidyl methacrylate benzaldehyde)<sub>0.25</sub>] (P2') in CDCl<sub>3</sub>.

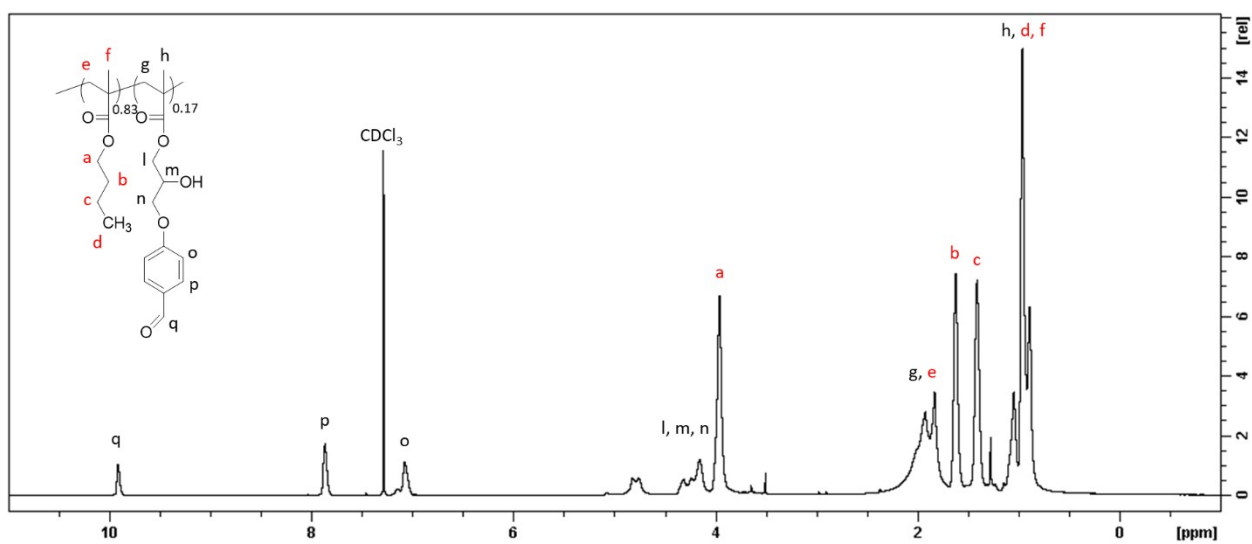


**Figure S11.** <sup>1</sup>H-NMR spectrum of aldehyde modified poly[(*n*-butyl methacrylate)<sub>0.83</sub>-*co*-(glycidyl methacrylate benzaldehyde)<sub>0.17</sub>] (P3') in CDCl<sub>3</sub>.

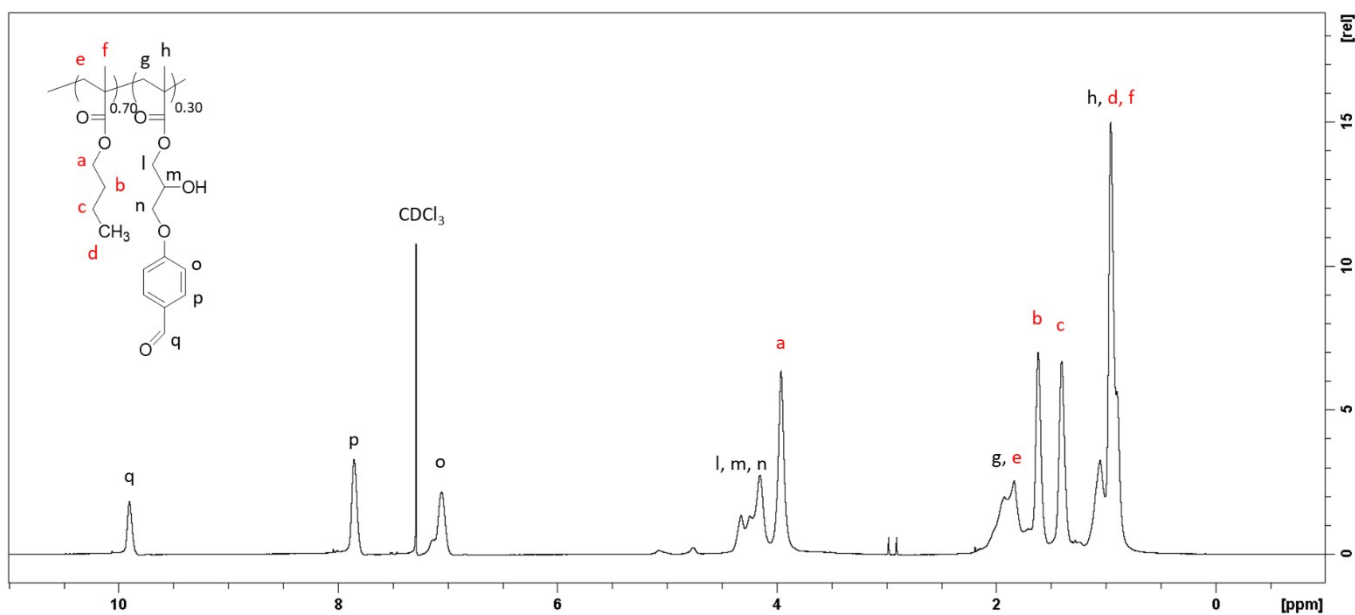


**Figure S12.**  $^1\text{H-NMR}$  spectrum of aldehyde modified poly[(*n*-butyl methacrylate) $_{0.70}$ -*co*-(glycidyl methacrylate benzaldehyde) $_{0.30}$ ] (P4') in  $\text{CDCl}_3$ .

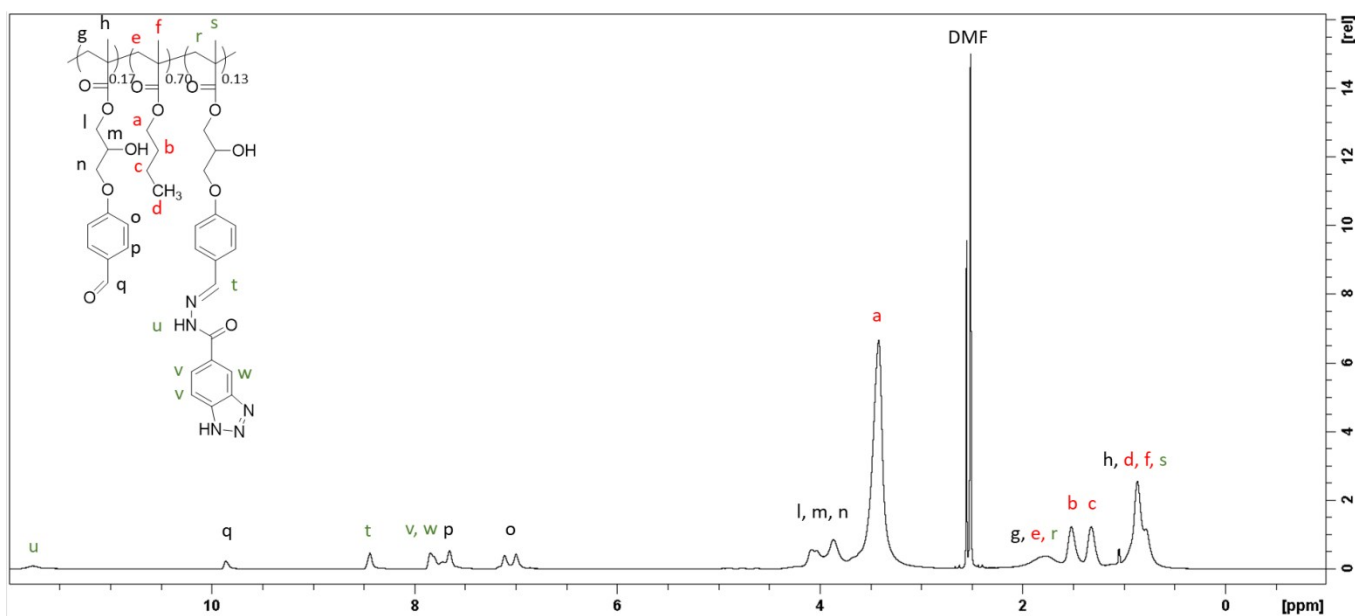


**Figure S13.**  $^1\text{H-NMR}$  spectrum of poly[(*n*-butyl methacrylate) $_{0.70}$ -*co*-(glycidyl methacrylate benzaldehyde) $_{0.17}$ -*co*-(glycidyl methacrylate benzaldehyde BTA) $_{0.13}$ ] (PBTA $_{0.13}$ ) in  $\text{DMSO}$ .

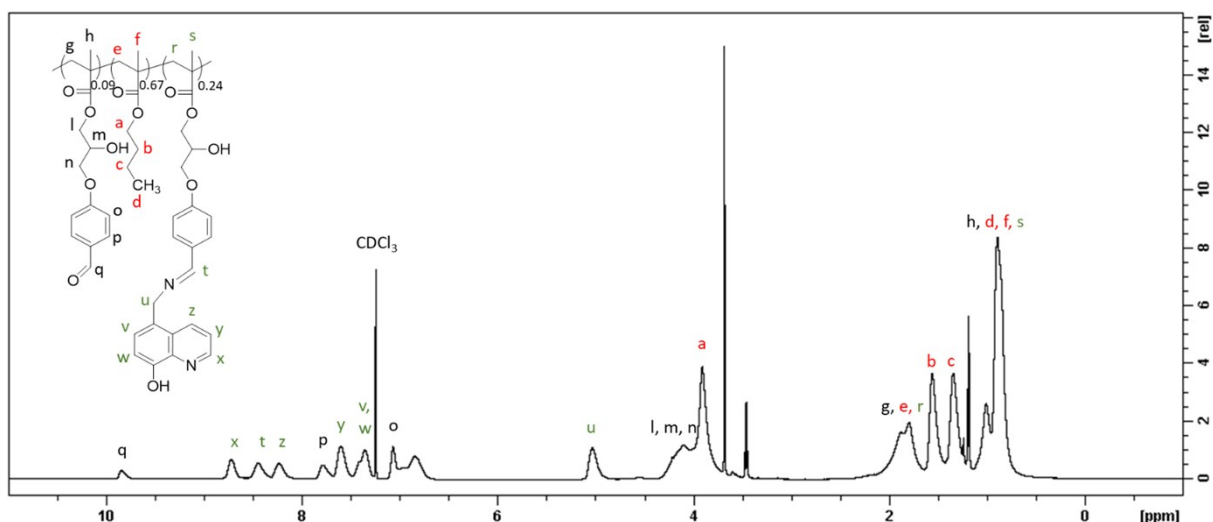


**Figure S14.** <sup>1</sup>H-NMR spectrum of poly[(*n*-butyl methacrylate)<sub>0.67</sub>-co-(glycidyl methacrylate benzaldehyde)<sub>0.09</sub>-co-(glycidyl methacrylate benzaldehyde AM8HQ)<sub>0.24</sub>] (PAM8HQ<sub>0.24</sub>) in CDCl<sub>3</sub>.

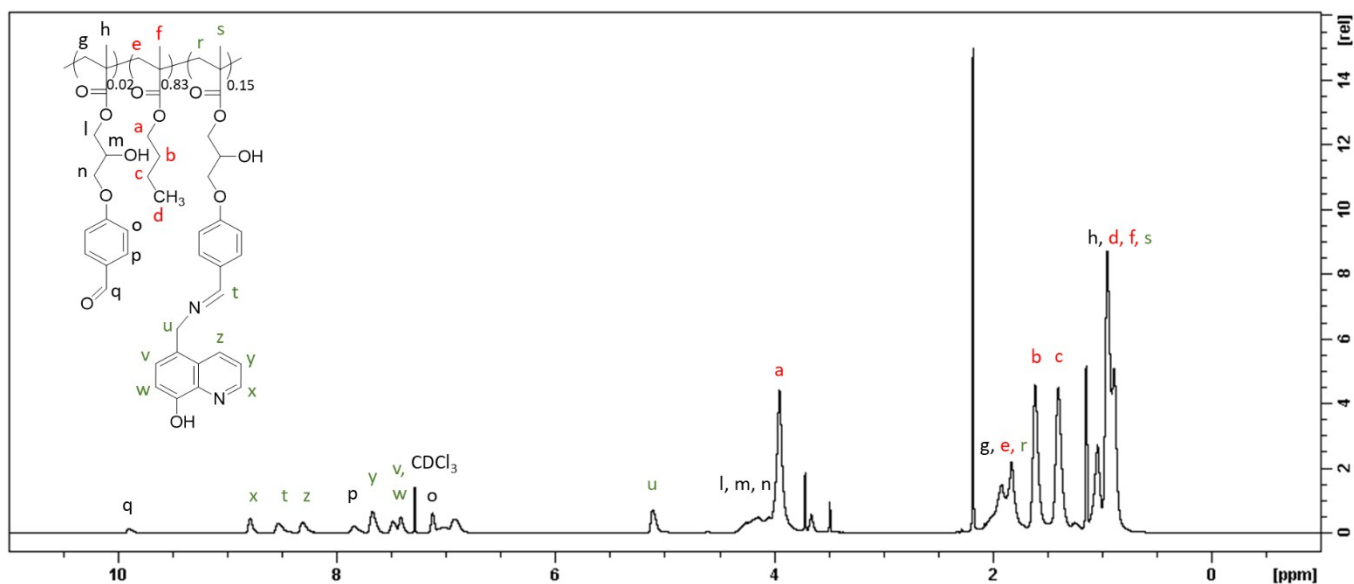


**Figure S15.** <sup>1</sup>H-NMR spectrum of poly[(*n*-butyl methacrylate)<sub>0.83</sub>-co-(glycidyl methacrylate benzaldehyde)<sub>0.02</sub>-co-(glycidyl methacrylate benzaldehyde AM8HQ)<sub>0.15</sub>] (PAM8HQ<sub>0.15</sub>) in CDCl<sub>3</sub>.

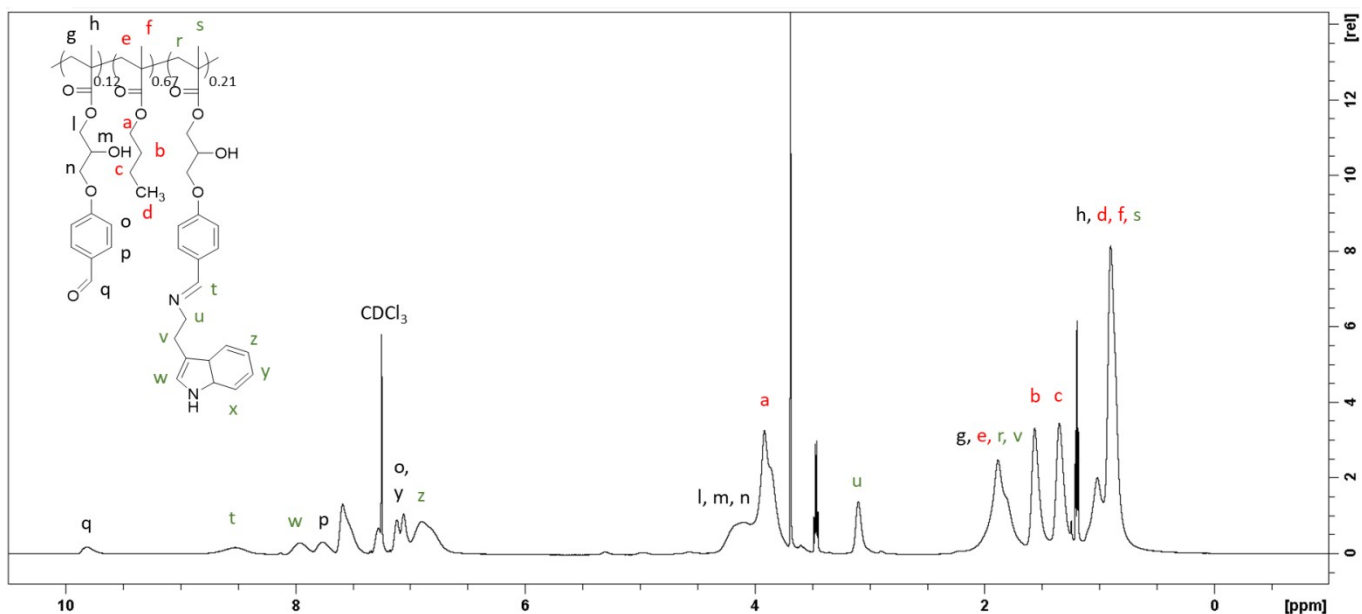


**Figure S16.**  $^1\text{H-NMR}$  spectrum of poly[(*n*-butyl methacrylate) $_{0.67}$ -*co*-(glycidyl methacrylate benzaldehyde) $_{0.12}$ -*co*-(glycidyl methacrylate benzaldehyde tryptamine) $_{0.21}$ ] (PTRY $_{0.21}$ ) in  $\text{CDCl}_3$

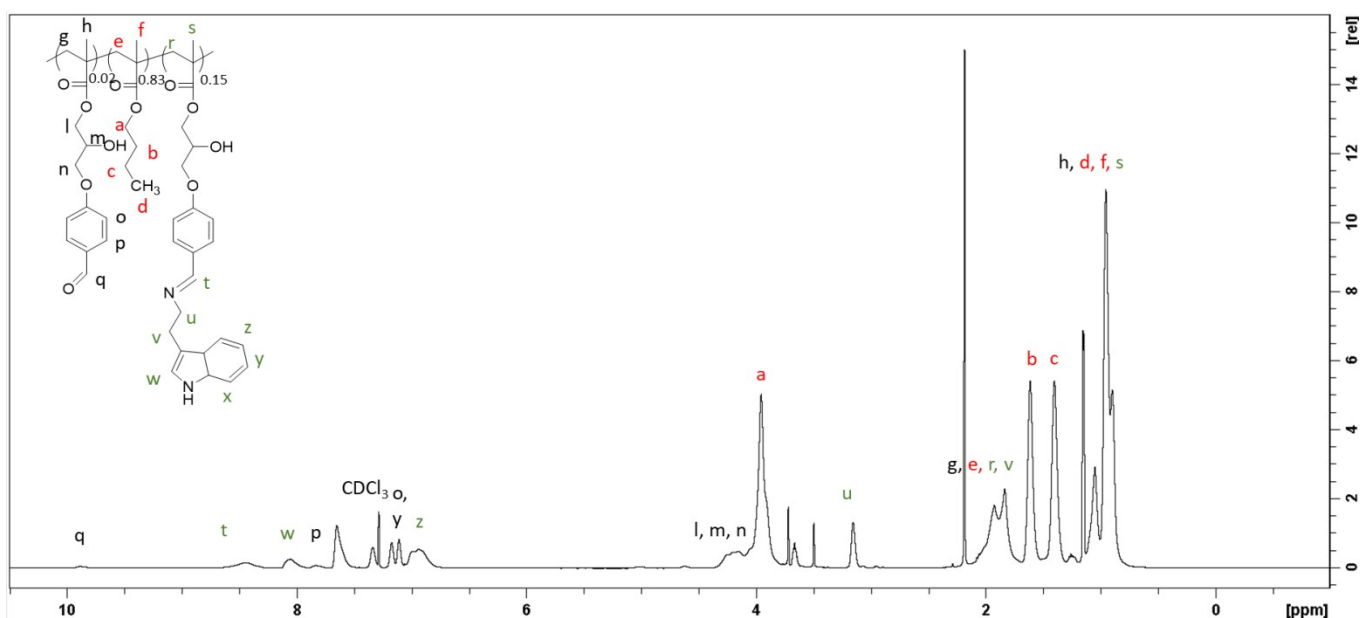


**Figure S17.**  $^1\text{H-NMR}$  spectrum of poly[(*n*-butyl methacrylate) $_{0.83}$ -*co*-(glycidyl methacrylate benzaldehyde) $_{0.02}$ -*co*-(glycidyl methacrylate benzaldehyde tryptamine) $_{0.15}$ ] (PTRY $_{0.15}$ ) in  $\text{CDCl}_3$

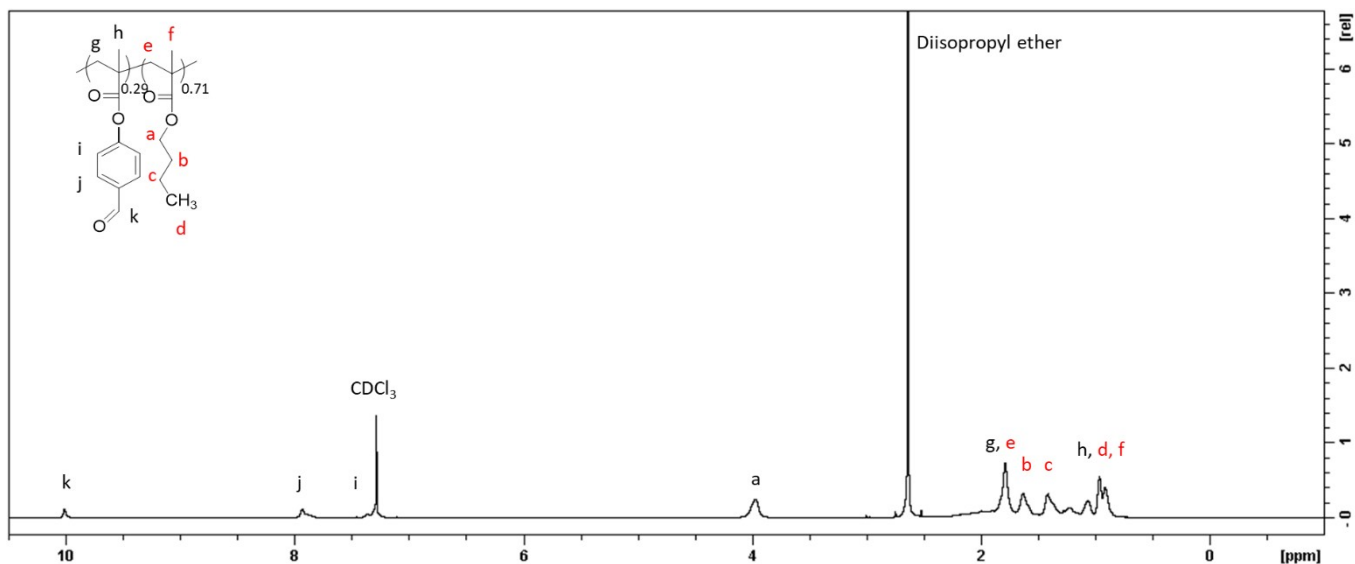


**Figure S18.**  $^1\text{H-NMR}$  spectrum of aldehyde modified poly[(*n*-butyl methacrylate) $_{0.71}$ -*co*-(4-formylphenyl methacrylate) $_{0.29}$ ] (P5) in  $\text{CDCl}_3$ .

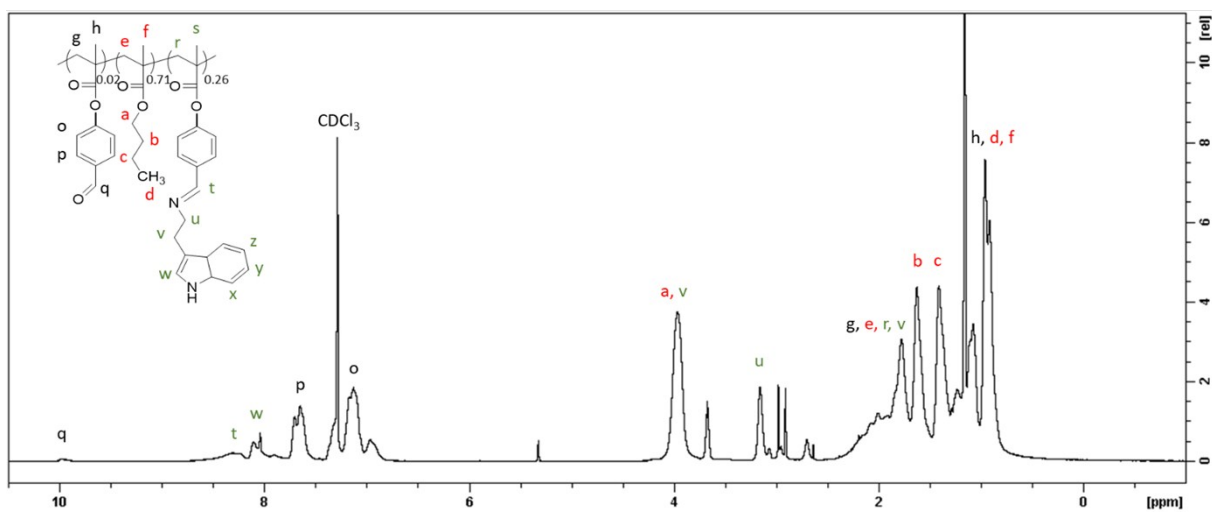


**Figure S19.**  $^1\text{H-NMR}$  spectrum of poly[(*n*-butyl methacrylate) $_{0.71}$ -*co*-(4-formylphenyl methacrylate) $_{0.03}$ -*co*-(4-formylphenyl methacrylate tryptamine) $_{0.26}$ ] (PFTRY $_{0.26}$ ) in  $\text{CDCl}_3$ .

## TGA experiments

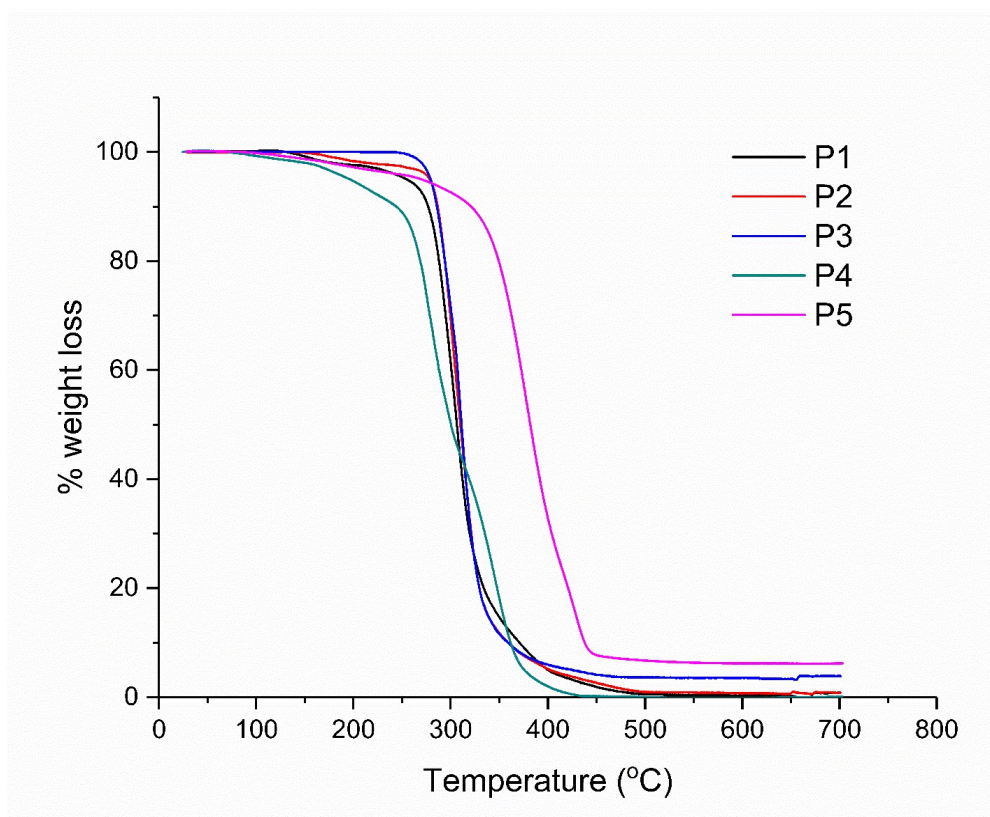


**Figure S20.** Thermogram displaying the thermal stability of poly[(*n*-butyl methacrylate)<sub>0.67</sub>-*co*-(glycidyl methacrylate)<sub>0.33</sub>] (P1), poly[(*n*-butyl methacrylate)<sub>0.75</sub>-*co*-(glycidyl methacrylate)<sub>0.25</sub>] (P2), poly[(*n*-butyl methacrylate)<sub>0.83</sub>-*co*-(glycidyl methacrylate)<sub>0.17</sub>] (P3), of poly[(*n*-butyl methacrylate)<sub>0.70</sub>-*co*-(glycidyl methacrylate)<sub>0.30</sub>] (P4), and poly[(*n*-butyl methacrylate)<sub>0.71</sub>-*co*-(4-formylphenyl methacrylate)<sub>0.29</sub>] (P5) .

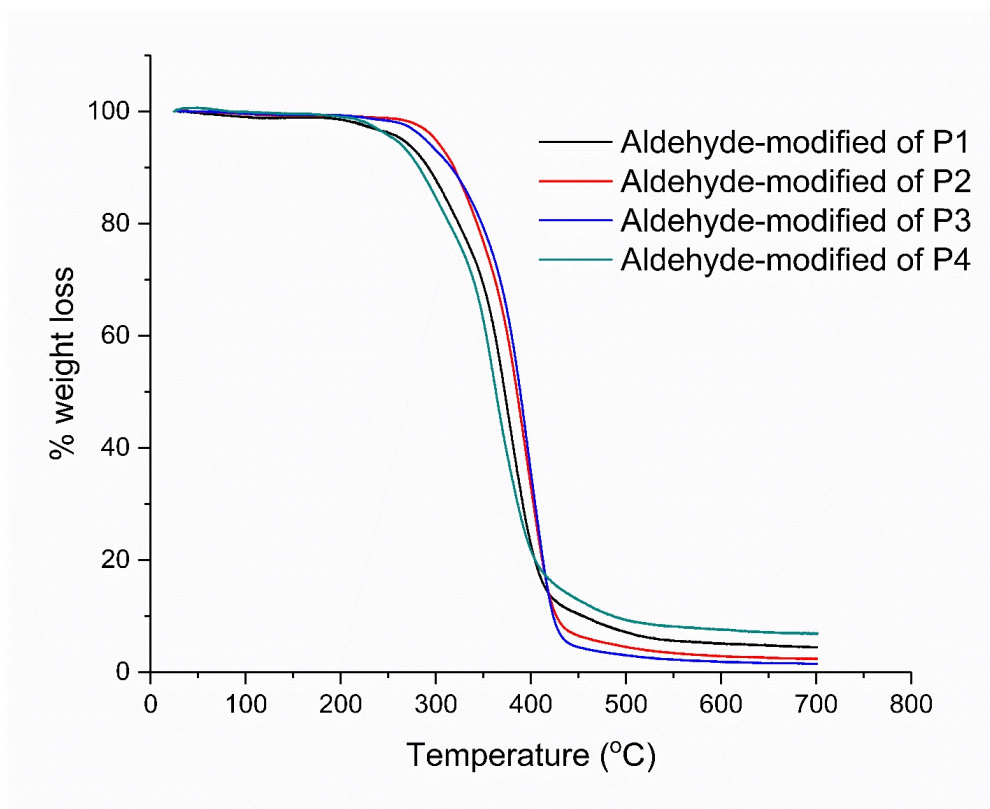


**Figure S21.** Thermogram displaying the thermal stability of aldehyde modified poly[(*n*-butyl methacrylate)<sub>0.67</sub>-*co*-(glycidyl methacrylate benzaldehyde)<sub>0.33</sub> (P1'), aldehyde modified poly[(*n*-butyl methacrylate)<sub>0.75</sub>-*co*-(glycidyl methacrylate benzaldehyde)<sub>0.25</sub> (P2'), aldehyde modified poly[(*n*-butyl methacrylate)<sub>0.83</sub>-*co*-(glycidyl methacrylate benzaldehyde)<sub>0.17</sub> (P3'), and aldehyde modified poly[(*n*-butyl methacrylate)<sub>0.70</sub>-*co*-(glycidyl methacrylate benzaldehyde)<sub>0.30</sub> (P4').

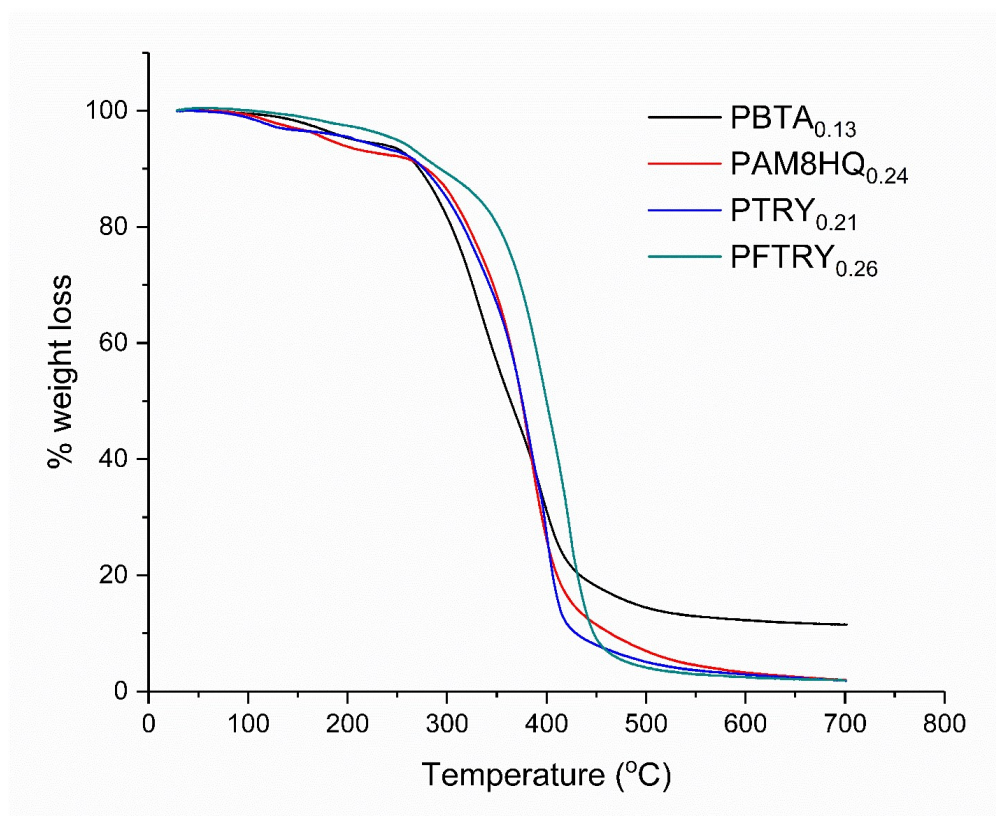


**Figure S22.** Thermograms displaying the thermal stability of poly[(*n*-butyl methacrylate)<sub>0.70</sub>-*co*-(glycidyl methacrylate benzaldehyde)<sub>0.17</sub>-*co*-(glycidyl methacrylate benzaldehyde BTA)<sub>0.13</sub>] (PBTA<sub>0.13</sub>), poly[(*n*-butyl methacrylate)<sub>0.67</sub>-*co*-(glycidyl methacrylate benzaldehyde)<sub>0.09</sub>-*co*-(glycidyl methacrylate benzaldehyde AM8HQ)<sub>0.24</sub>] (PAM8HQ<sub>0.24</sub>), poly[(*n*-butyl methacrylate)<sub>0.67</sub>-*co*-(glycidyl methacrylate benzaldehyde)<sub>0.12</sub>-*co*-(glycidyl methacrylate benzaldehyde tryptamine)<sub>0.21</sub>] (PTRY<sub>0.21</sub>), and poly[(*n*-butyl methacrylate)<sub>0.71</sub>-*co*-(4-formylphenyl methacrylate)<sub>0.03</sub>-*co*-(4-formylphenyl methacrylate tryptamine)<sub>0.26</sub>] (PFTRY<sub>0.26</sub>).

## SEM measurements

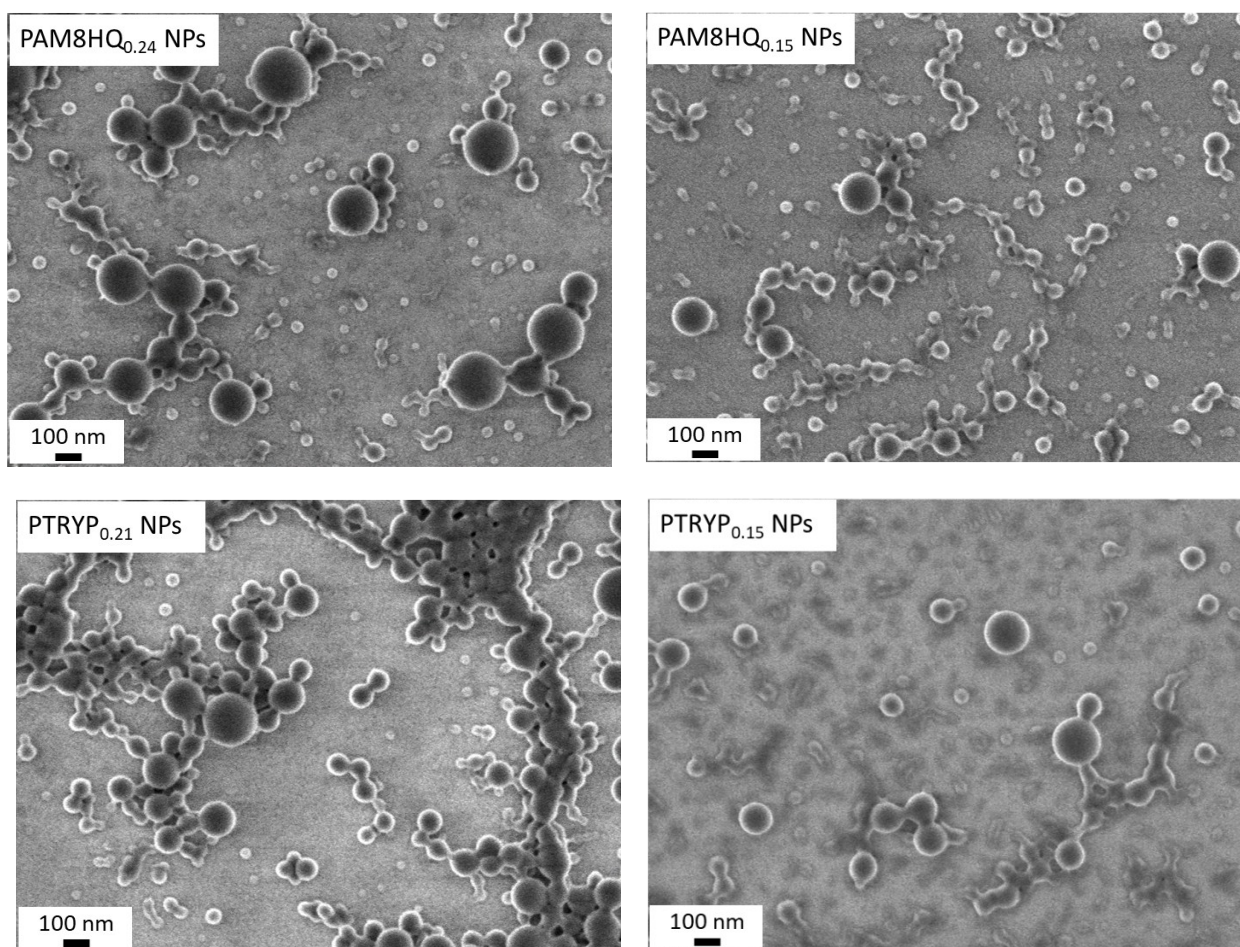


**Figure S23.** SEM micrographs of a) PAM8HQ<sub>0.24</sub> and PAM8HQ<sub>0.15</sub> nanoparticles and b) PTRY<sub>0.21</sub> and PTRY<sub>0.15</sub> nanoparticles.

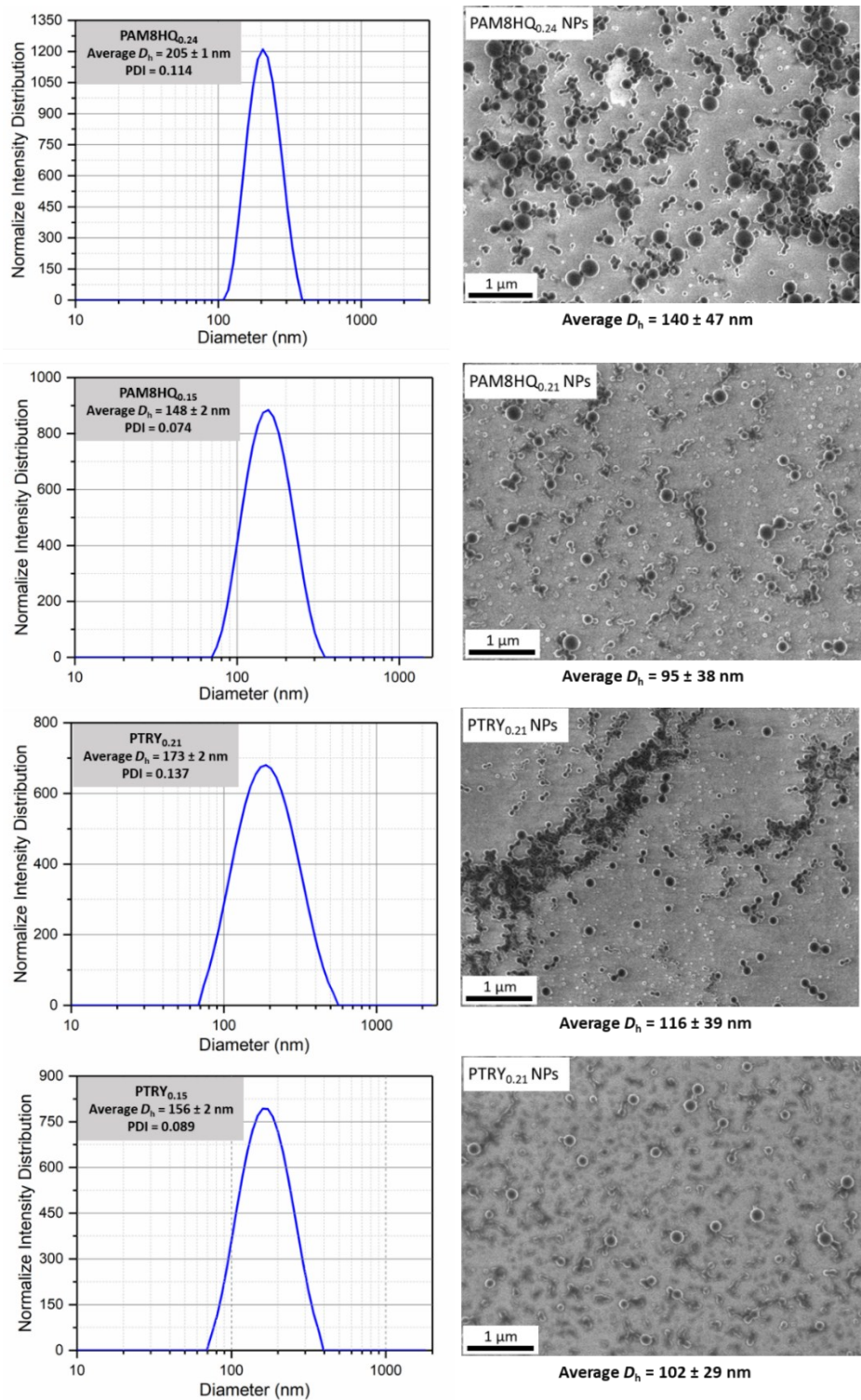


**Figure S24.** DLS analysis and SEM micrographs of PAM8HQ<sub>0.24</sub>, PAM8HQ<sub>0.15</sub>, PTRY<sub>0.24</sub>, and PTRY<sub>0.15</sub> nanoparticles.

## NMR spectra

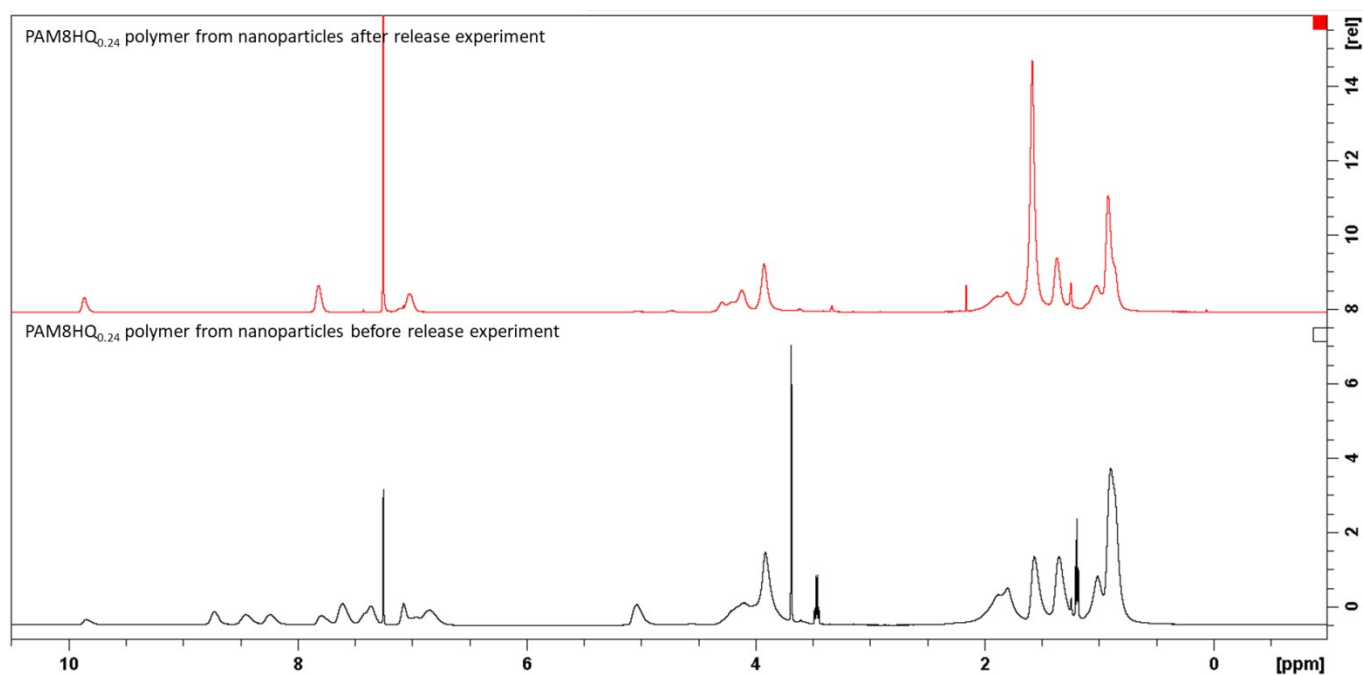


**Figure S25.** <sup>1</sup>H-NMR spectra of PAM8HQ<sub>0.24</sub> nanoparticles before and after release experiment in CDCl<sub>3</sub>.

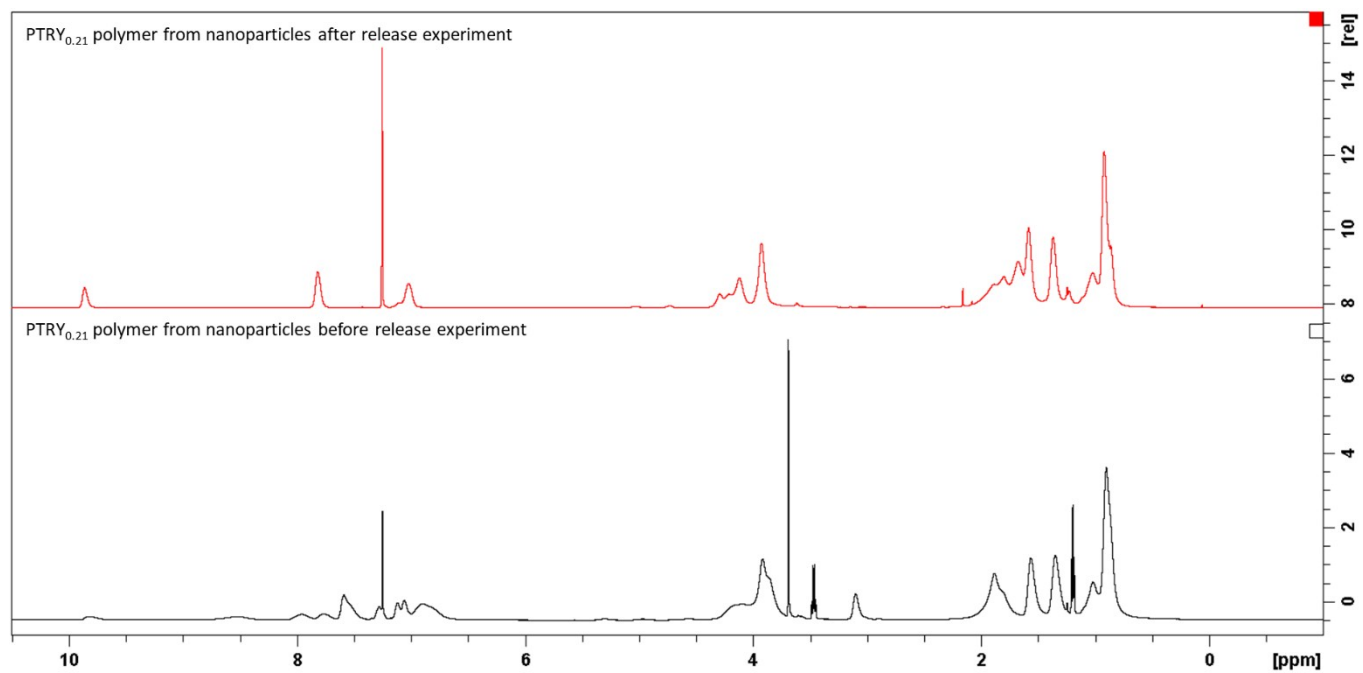


**Figure S26.** <sup>1</sup>H-NMR spectra of PTRY<sub>0.21</sub> nanoparticles before and after release experiment in CDCl<sub>3</sub>.

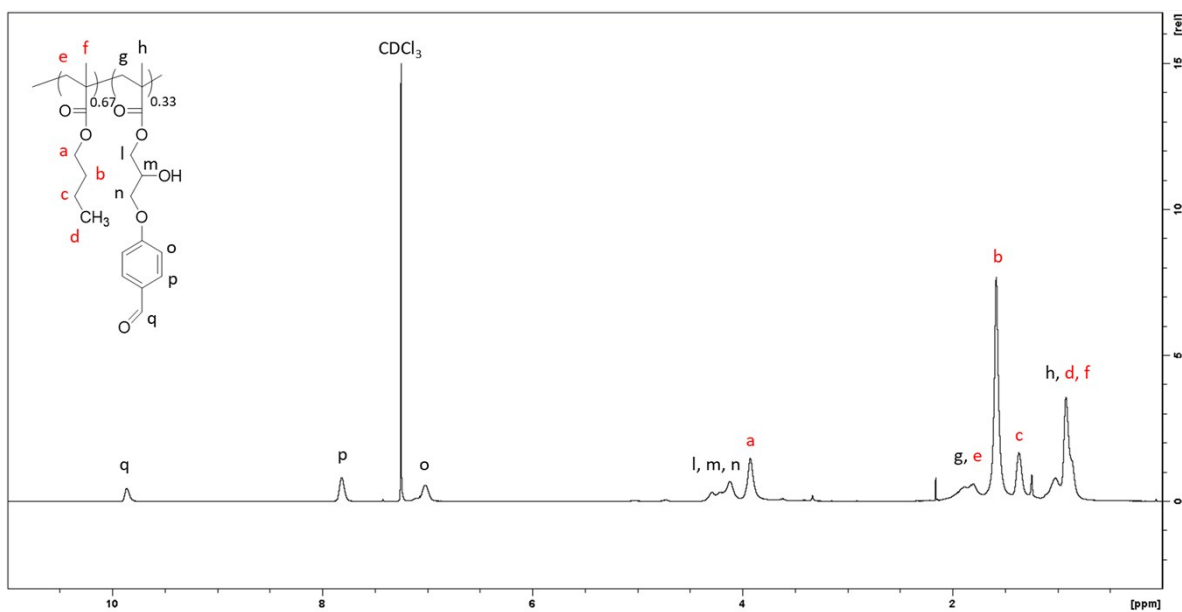


**Figure S27.**  $^1\text{H-NMR}$  spectrum of PAM8HQ<sub>0.24</sub> nanoparticles dissolved in  $\text{CDCl}_3$  after the release experiment in buffer solution at pH 3.5.

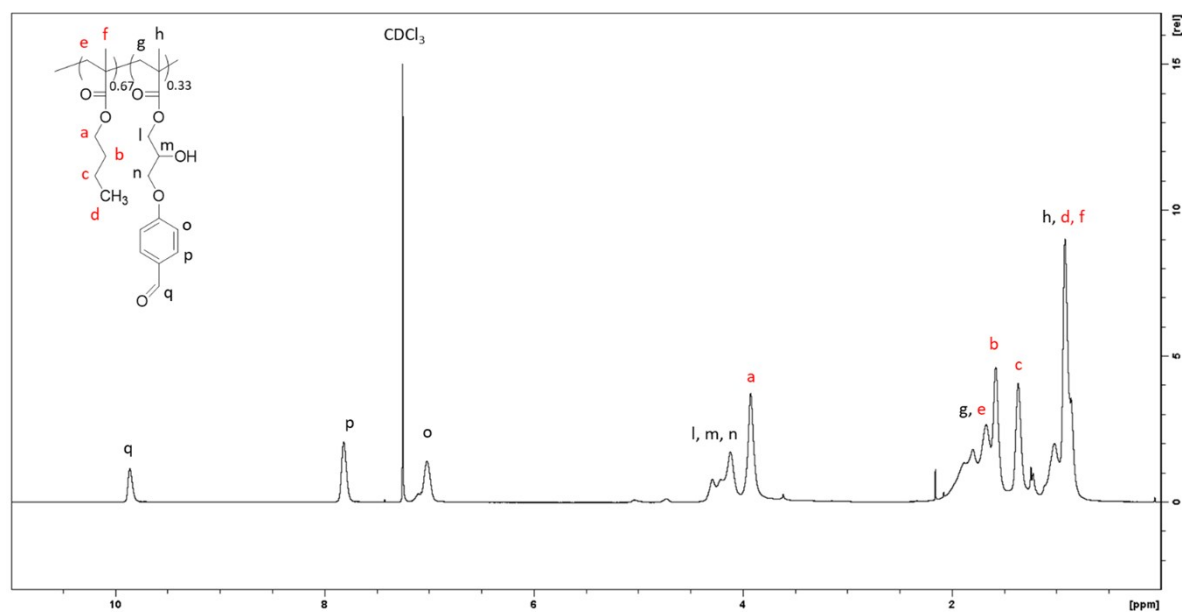


**Figure S28.**  $^1\text{H-NMR}$  spectra of PTRY<sub>0.21</sub> nanoparticles dissolved in  $\text{CDCl}_3$  after the release experiment in buffer solution at pH 3.5.

## Release kinetics model

### Equation 1

$$F = K_{KP}(t - T_{lag})^n$$

F = fraction (%) of drug released in time t

$K_{KP}$  = release rate constant

$T_{lag}$  = lag time before the release process starts

n = diffusional exponent indicating the drug-release mechanism

$n \leq 0.43$  for classical Fickian diffusion-controlled release

$0.43 < n < 0.85$  for a non-Fickian diffusion release that refers to a combination of diffusion and the polymer relaxation mechanism

$n > 0.85$  for a non-Fickian diffusion release or Zero order release

**Table S1.** Correlation coefficient  $R^2$ , release rate constant  $K_{KP}$ , lag time  $T_{lag}$ , and diffusional exponent  $n$  obtained by fitting the release curves with the Korsmeyer-Peppas model.

Nanoparticles	pH	$R^2$	$K_{kp}$	$T_{tag}$	n
PTRY <sub>0.21</sub>	3.5	0.9894	42.9142	19.6656	0.0982
	7	0.9803	13.7309	55.0784	0.2121
PTRY <sub>0.15</sub>	3.5	0.9864	32.7094	9.9880	0.1257
	7	0.9620	12.0851	19.4923	0.2320
PFTRY <sub>0.26</sub>	3.5	0.9908	5.4664	27.5291	0.3067
	7	0.9969	0.3498	3.1813	0.4287

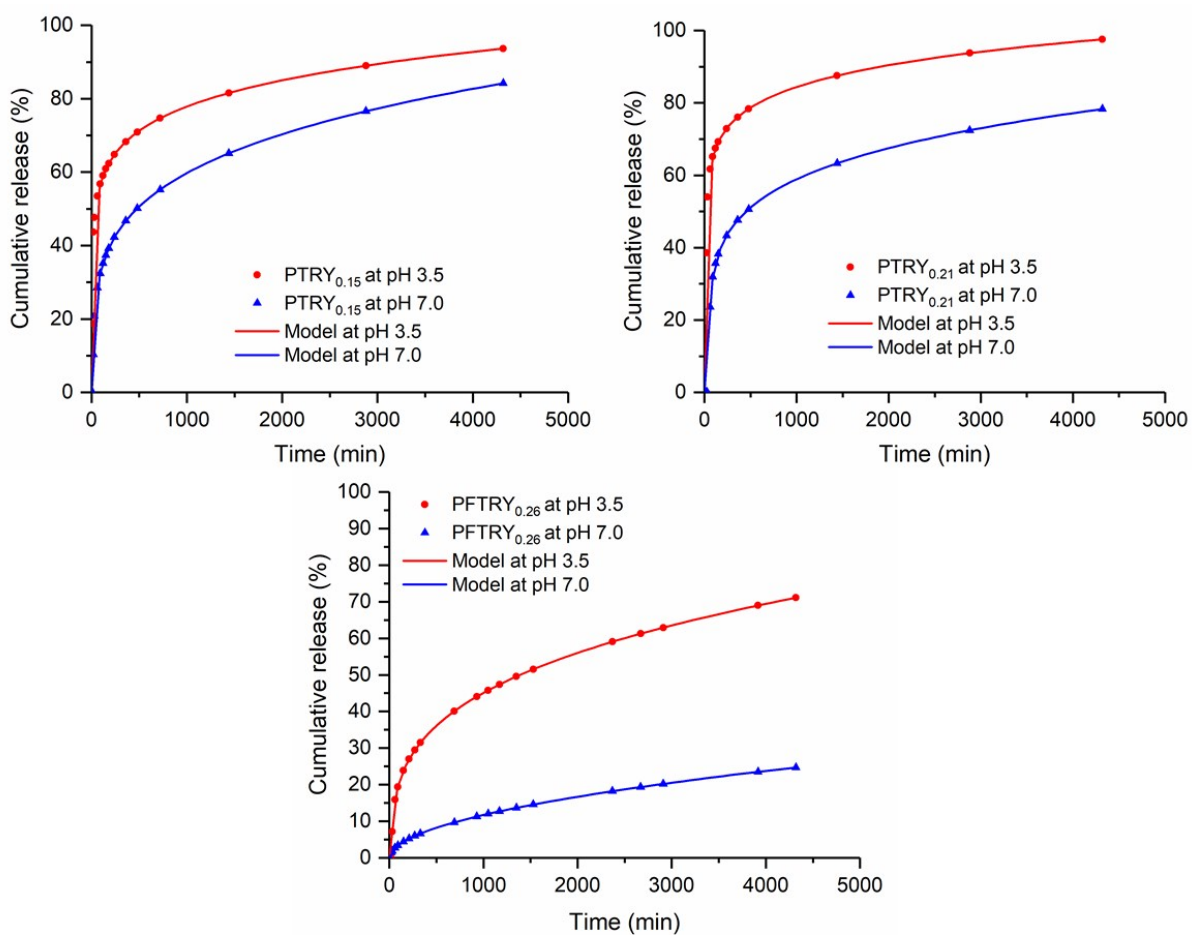


**Figure S29.** Release profile of tryptamine from nanoparticles of PTRY<sub>0.21</sub>, PTRY<sub>0.15</sub>, and PFTRY<sub>0.26</sub> nanoparticles at pH 3.5 and 7.0 fitted with the Korsmeyer-Peppas model.

## Anticorrosion performance

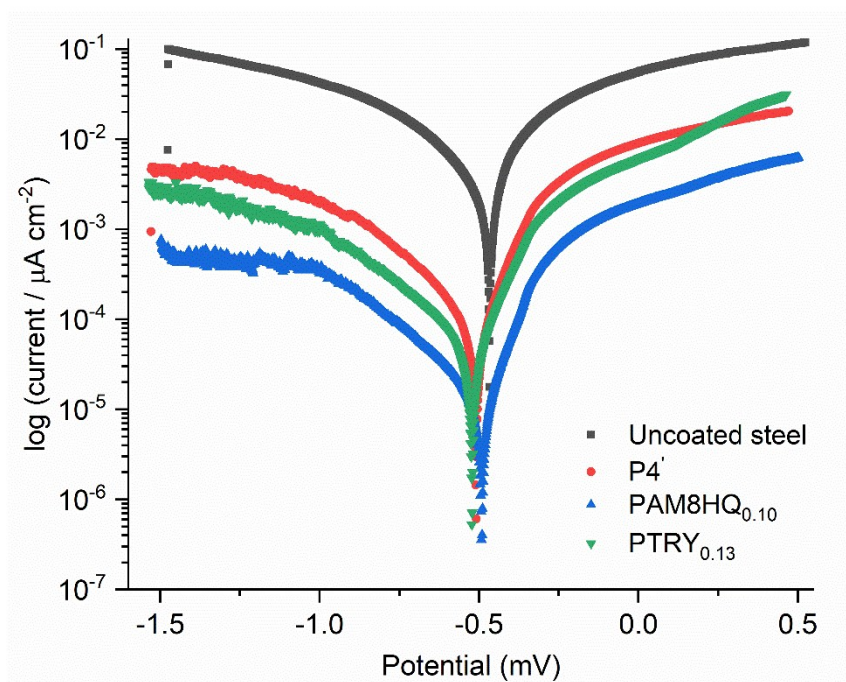


**Figure S30.** Tafel plots of uncoated steel and steel coated with P4', PAM8HQ<sub>0.10</sub>, and PTRY<sub>0.13</sub> in 0.1 M HCl aqueous solution.